JOURNAL OF CATALYSIS 141, 114–123 (1993)

Sol–Gel Ru/SiO_2-Catalysts: Theoretical and Experimental Determination of the Ru-in-Silica Structures

T. LÓPEZ,*,[1] R. GÓMEZ,*,[1] O. NOVARO,* A. RAMÍREZ-SOLÍS,† E. SÁNCHEZ-MORA,† S. CASTILLO,† E. POULAIN,† AND J. M. MARTÍNEZ-MAGADÁN†

Instituto de Física, UNAM, Apartado Postal 20-364, 01000 México, Distrito Federal; and †Instituto Mexicano del Petróleo, Gerencia de IBP, Apartado Postal 14-805, México 07730 Distrito Federal

Received September 14, 1992; revised December 8, 1992

Preparation of Ru/SiO_2 catalysts with sol–gel techniques allows better selectivity and much greater resistance to coke formation and deactivation than the traditional impregnation method. This has been attributed to the incorporation of Ru into the silica network for the sol–gel catalyst. To further understand the structure of the Ru occluded in the silica network, a variety of spectroscopical studies and quantum mechanical calculations were carried out, confirming previously proposed structures and showing good agreement between the theoretical and experimental results. © 1993 Academic Press, Inc.

1. INTRODUCTION

In previous papers (*1*, *2*), we presented a comparison between Ru/SiO_2 catalysts prepared by impregnation and by sol–gel preparation methods. It was concluded that for the *o*-xylene hydrogenation the sol–gel catalysts showed a much higher resistance to deactivation and substantially enhanced selectivity (*1*). Mechanical stability was also improved for sol–gel Ru catalysts (*2*), Ru is stabilized by its incorporation into the silica framework and does not sinter or volatilize following treatment in O_2 at temperatures up to 450°C. These advantages were attributed to the incorporation of ruthenium in the silica framework, which only occurs for the catalysts prepared by the sol–gel method. A suggested structure for the Ru atoms in the network was advanced (*1*), and in fact other authors (*3*) have proposed alternative structures for metal occlusion in silica. The aim of the present paper is to study carefully these structures which may turn out to play a decisive role for improved catalysts.

Before that, let us review briefly the sol–gel (*4*) technique as applied to the preparation of catalytic material. The method consists on the hydrolysis and condensation of metallic alkoxides to polymerize in microporous and nonbranched structures. The silica support, for instance, can be prepared as follows:

Hydrolysis

$$Si(OEt)_4 + H_2O \rightarrow HO - Si(OEt)_3 + EtOH.$$

Condensation

$$\equiv Si{-}OEt + \equiv Si{-}OH \rightarrow \equiv Si{-}O{-}Si\equiv + EtOH$$

$$\equiv Si{-}OH + \equiv Si{-}OH \rightarrow \equiv Si{-}O{-}Si\equiv + HOH.$$

This technique of preparation is particularly valuable because the physical and chemical properties of the final solid can be controlled from the beginning and throughout the synthesis. Furthermore, it allows

[1] Permanent address: Universidad Autónoma Metropolitana-Iztapalapa, Apartado Postal 55-534, México, D.F. 09340.

0021-9517/93 $5.00

the incorporation of the catalytically active metals (in our case ruthenium) and ensures a direct metal–support interaction (*5–7*). The metal–support interaction itself has received increasing interest in the literature (*8–10*), but in the case of Ru (a metal particularly active for Fisher–Tropsch synthesis (*11*), methanation (*12*), CO oxidation (*13*), hydrogenation, and other hydrocarbon reactions (*14*)), metal–support interactions have additional interest. This is due to the well-known tendency of Ru to evolve in time and specially to form coke, which leads to rapid deactivation (*15*). Considering that deactivation stems from partially dehydrogenated aromatic hydrocarbon rings polymerizing on the active sites, the sol–gel method has the advantage of generating structures that inhibit the blocking of Ru sites due to the formation of small isles of Ru/SiO_2–OH on the surface of the metallic particles. Consequently, the OH groups in the surface are expected to surround the highly disperse metal particles, preventing the deactivation which inevitably occurs on traditionally prepared impregnation catalysts (*1*).

To study the role played by the OH groups in the surface as well as the structures of the occluded Ru within the silica network, we shall here present two types of studies: diffuse-reflectance spectroscopic experiments and quantum-chemical calculations. The details of both methods are reported in the following section.

2. METHOD

(*a*) *Experimental*

The detailed description of the experimental techniques has been given before (*1*). We shall only present a brief summary here. The sol–gel process includes varying concentrations of Ru on the silica support, 0.5, 1.0, and 2.0%, leading to catalysts labeled Ru-0.5, Ru-1, and Ru-2. An adequate amount of $RuCl_3 \cdot 3H_2O$ (ICN K & K Inc., 99.9%), is refluxed at 70°C with 10 ml of H_2O and 10 ml of absolute ethanol (Baker 99.9%) with permanent agitation. Afterwards, 37 ml of tetraethoxysilane (TEOS) are added drop by drop. The reflux continues until the (Ru-0.5) gel is formed. The Ru-1 and Ru-2 catalysts are similarly obtained varying the Ru percentage accordingly. The gels are dryed at 70°C for 12 h and then are treated at 300 and 600°C during 24 h. Thermogravimetric (TGA) and differential thermal (DTA) analyses were carried out in an N_2 atmosphere in a Shimetzu apparatus.

Catalytic activity is measured on the benzene hydrogenation at atmospheric pressure and 100°C temperature. Reaction rates are obtained under these conditions. Partial pressures for benzene and hydrogen are 14.0 and 760 Torr, respectively. The gas analysis was carried out using a gas chromatograph; under these conditions the only detected product was cyclohexane. BET areas are measured in a Micromeritics 2300 model. The spectroscopic characterization is obtained using a Varian Model 7-D for the UV–Vis spectra.

(*b*) *Theoretical*

The possibility of determining the structure of a molecule before its synthesis, or that of a hard-to-detect intermediate, etc., is quite tempting. The laws of quantum mechanics can in principle provide this information. In truth, the sheer complexity of the systems involved in catalytic processes makes this a highly difficult task. A complete study of a catalytic reaction using empirical (*16*) and even fully *ab initio* (*17*) quantum mechanical techniques has occasionally been achieved. The Ru/SiO_2 system studied here, however, has its particular difficulties. We are interested in the configuration that the Ru occluded in the silica network might have. In Fig. 10 of Ref. (*1*) a specific proposal for this configuration is made which implies a Ru/SiO_2 structure involving the coordination of a Ru atom with two edges and two vertex of the SiO_4 tetrahedra. Here we reproduce this figure as Fig. 1. Other authors (*3*) have proposed that metals in silica coordinate with three edges in the configuration schematized in Fig. 2. To decide which of

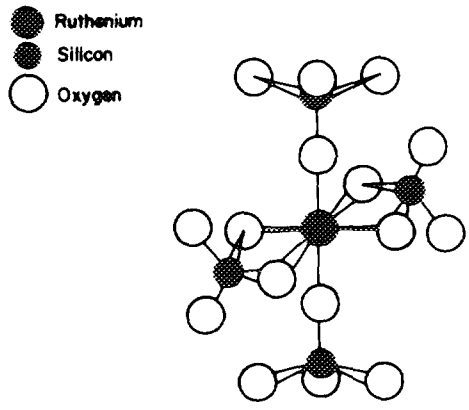

FIG. 1. Proposed coordination of Ru in silica.

these two structures is the most stable, the theoretical calculations have to be at an *ab initio* level, because only at this level the quantum mechanical results have absolute predictive value.

On the other hand, *ab initio* calculations are too time and space-consuming to attempt to study more than the immediate neighbors of the occluded Ru. Therefore, to study the effects that the metal introduces in the silica network as a whole and compare with experiment, we introduced another theoretical approach, simpler, with less independent predictive power, but capable of encompassing a substantial part of the Ru-containing silica, in other words, a semiempirical calculation.

In short, the theoretical results are twofold. On the one hand, we have *ab initio* Self Consistent Field (SCF) calculations of the immediate coordination shell of Ru, using the PSHF program of Toulouse (*18*) with basis sets and pseudopotentials used and reported in previous studies on the RuH_2 system (*19*). The reader is kindly referred to (*18*, *19*) for details. On the other hand, EH (extended-Hückel) calculations were addressed to a representative part of the silica network (dozens of atoms) containing the trapped Ru atoms. The latter utilized the EH program of Roald Hoffmann (*20*).

3. RESULTS

(*a*) *Theoretical*

As mentioned in the previous section, the *ab initio* calculation were addressed only to the immediate coordination sphere of Ru (i.e., the Ru–O bonds) in both structures of Figs. 1 and 2. Only SCF results are reported here, but correlation effects obtained through extensive configuration interaction apparently do not change the present conclusions (*21*). The structure of Fig. 1 implies the interaction of Ru with two vertex and two edges of the SiO_4 tetrahedra, that of Fig. 2 with three edges. The total SCF energy of both structures is more favorable towards the structure of Fig. 1 by 14.4 kcal/mol. More details can be found in (*22*). These theoretical results back up the proposal (*1*) of the structure of Fig. 1. We should remember that this proposal was soundly based on extensive X-ray results. It is interesting to note that when ruthenium–oxygen bonds are formed they involve low-multiplicity states of the metal and, in fact, the orbital analysis of the metal–oxygen complex shows a series of symmetry-avoided crossings as has been established for several transition metals (*23*).

Continuing with the theoretical calculations we now present the EH calculations on the structure of the silica and the modifi-

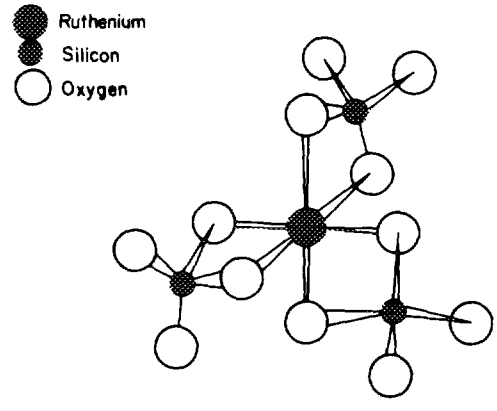

FIG. 2. Previously proposed (*3*) coordination of Ru in silica.

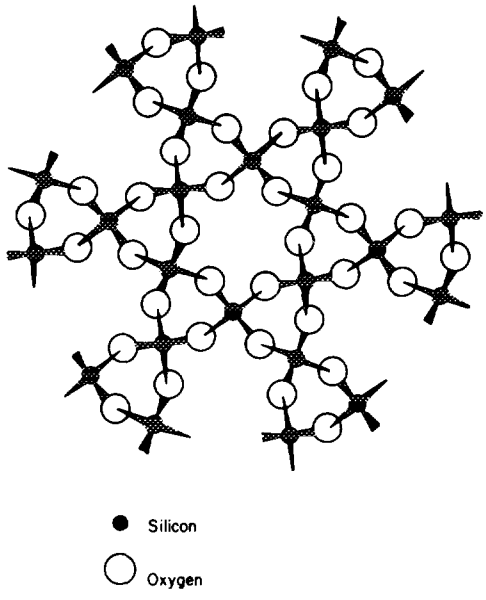

FIG. 3. The β-quartz network.

cations thereof by the occlusion of Ru in the network. First of all, we must choose the silica structure, which at atmospheric pressure may adopt three crystalline forms, which are stable in the temperature ranges

$$\xrightarrow[\text{quartz}]{} 870°C \xleftrightarrow[\text{tridimite}]{} 1470°C \xleftrightarrow[\text{cristalobite}]{} 1710°C.$$

Considering the range of temperatures used in this and previous (*1*, *2*) studies, we conclude that the structure at 600°C that would interest us would be quartz, which is depicted in Fig. 3 as a system of SiO_4 tetrahedra in a helix-like distribution. Figure 3 depicts the β-form of quartz. The corresponding bond lengths are given in Table 1; α-quartz is a distorted version thereof (the transition temperature of both forms of quartz is 573°C). We shall use a β-quartz structure and allow an Ru atom to enter it and analyze the deformation induced by the metal.

Quartz has an hexagonal-trapezoidal structure-622. Its space group is $C6_22(D_6^4)$. Its unit cell contains three Si and six oxygen atoms. The dimensions of its unit cell are $\alpha_0 = 4.999$ Å and $C_0 = 5.457$ Å according to (*24*) and $\alpha_0 = 5.01$ Å and $C_0 = 5.47$ Å according to (*25*). The spatial location of the three SiO_2 in the unit cell are

$$\text{Si: } \tfrac{1}{2}, \tfrac{1}{2}, \tfrac{1}{2};\quad \tfrac{1}{2}, 0, 0;\quad 0;\quad \tfrac{1}{2}; \tfrac{2}{3}$$

$$\text{0: } u, u, \tfrac{5}{6};\quad u, 2u, \tfrac{1}{2};\quad 2u, u, \tfrac{1}{6}$$

(with $u = 0.197$) which is represented in Fig. 4.

TABLE 1

Interatomic Bond Distances of Ru in β-Quartz (See Fig. 5)

Atom number	Bond	Distance (Å)	Atom number	Bond	Distance (Å)
1–2	Ru–Si	4.07	25–23	O–O	3.46
1–6	Ru–Si	3.20	25–4	O–O	2.22
1–3	Ru–O	3.45	25–3	O–O	3.25
1–23	Ru–O	2.40	23–3	O–O	2.22
2–3	Si–O	1.83	23–4	O–O	3.48
2–4	Si–O	1.93	3–4	O–O	3.47
2–23	Si–O	1.93	3–5	O–O	4.02
2–25	Si–O	1.83	3–7	O–O	4.02
6–3	Si–O	4.33	3–8	O–O	5.51
6–5	Si–O	2.10	5–7	O–O	3.86
6–7	Si–O	2.10	5–8	O–O	2.80
6–8	Si–O	1.42	7–8	O–O	2.80
2–6	Si–Si	4.18	4–5	O–O	2.64
6–10	Si–Si	4.07			

The bond lengths of Table 1 were used in EH calculations on the structure of Fig. 3. Each Si atom was given a charge of +4 and −2 for each 0. Then an Ru atom was added in the center of the structure to see how it deformed the β-quartz structure in its immediate vicinity. To see if the choice of the charge in the Ru atom affected the results,

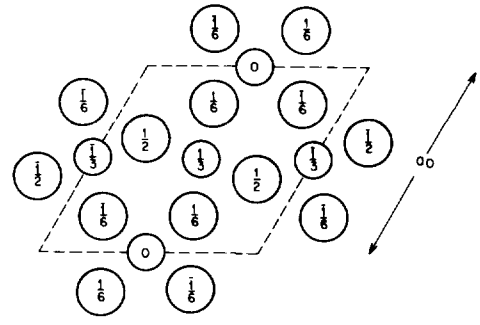

FIG. 4. Unit cell of β-quartz. Small circles silicon and large circles oxygen.

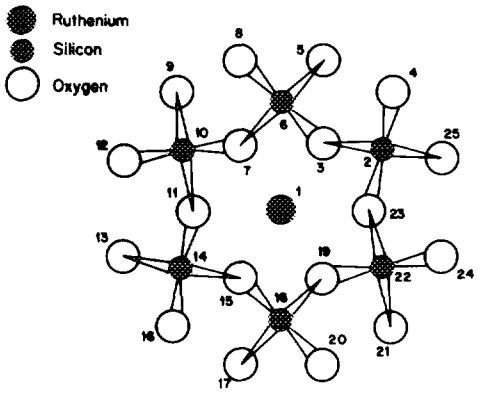

FIG. 5. $Ru-Si_6O_{18}$ model cluster used for the EH calculations.

two values were given to the charge in ruthenium, 0 and +4.

The EH calculations on the structure of Fig. 3 gave the following charges: $Si_{1,2} = 2.41$, $Si_{3,4} = 2.34$, and $Si_{5,6} = 2.11$; $O_{1,2} = -1.57$, $O_{3,4} = -1.63$, $O_{5,6} = 1.60$, $O_{7,8} = -1.26$, $O_{9,10} = -1.15$, $O_{11,12} = -1.36$, $O_{13,14} = -1.03$, $O_{15,16} = -1.68$, and $O_{17,18} = -1.57$. (Note that the electronic charge is smaller for the internal oxygens.)

The introduction of Ru is depicted in Fig. 5. The charges of Si were virtually unchanged and the O charges only changed for the inner oxygens $O_{3,4} = 1.13$, $O_{7,8} = 1.11$, and $O_{17,18} = 1.11$. These values were for Ru with zero charge but introducing a Ru with charge +4 gave exactly the same charges at the Ru and Si centers as that with zero charge, showing that the formal charge in the metal does not affect the final charge distribution in the silica structure.

This charge distribution was obtained for the structure of Fig. 5 leaving the Si and O positions fixed at their experimental values for β-quartz (*24*, *25*). Then we allowed a reoptimization of the all of the bond lengths of Fig. 5, which permits us to assess the effects of Ru on the SiO_2 support. The reoptimized distances are reported in Table 2, which interestingly shows a systematic contraction of all the bond lengths in the neighborhood of the Ru, as a comparison with the distances of Table 1. When this contraction occurs the charge distribution does change, diminishing substantially at the Ru and Si. This is logical, considering that complete reoptimization of all distances in Table 2 allows the corresponding optimization of the individual bonds. This ensures the growth of the covalent distributions to the bonding situation with a concomitant reduction of the ionic distributions.

On the other hand the contraction of the β-quartz structure around the Ru manifest in Table 2 is in quite good agreement with experiment. The X-ray results for the Ru/SiO_2 sol–gel catalysts also have important contractions as reported in Ref. (*1*). The average Si–Si distance in our calculations is 4.02 Å, a result which differs less than 0.1 Å from the experimental average and our Si–O separations are also very close to experiment. The Ru–O distances however, are slightly overestimated by our calculations (approximately by ¼ Å).

(*b*) *Experimental*

Our new ultraviolet–visible (diffuse reflectance) spectra for the sol–gel catalysts are reported in Figs. 6 and 7. Figure 6 shows the spectra of the catalyst with varying Ru concentration: Ru-0.5, Ru-1, and Ru-2. After having been dried at 70°C, they have

TABLE 2

Optimized Interatomic Bond Distances of Ru in β-Quartz (Atomic Numbering Is that of Fig. 5)

Atom number	Bond	Distance (Å)	Atom number	Bond	Distance (Å)
1–2	Ru–Si	3.56	25–23	O–O	2.75
1–6	Ru–Si	2.97	25–4	O–O	2.22
1–3	Ru–O	3.37	25–3	O–O	2.34
1–23	Ru–O	2.32	23–3	O–O	2.22
2–3	Si–O	1.11	23–4	O–O	2.60
2–4	Si–O	1.74	3–4	O–O	2.43
2–23	Si–O	1.69	3–5	O–O	3.87
2–25	Si–O	1.48	3–7	O–O	3.91
6–3	Si–O	4.57	3–8	O–O	5.30
6–5	Si–O	1.73	5–7	O–O	2.79
6–7	Si–O	1.93	5–8	O–O	2.02
6–8	Si–O	1.13	7–8	O–O	2.53
2–6	Si–Si	4.49	4–5	O–O	2.91
6–10	Si–Si	3.56			

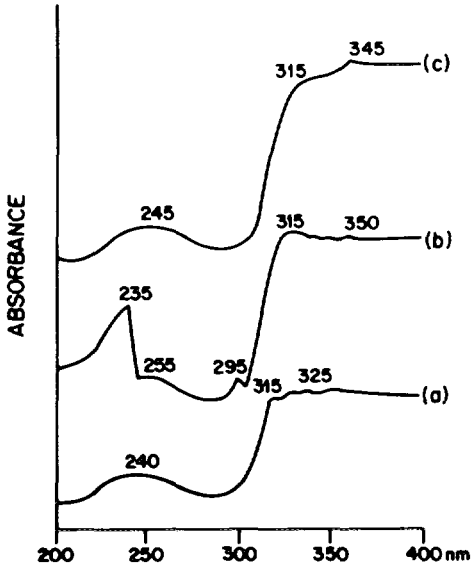

FIG. 6. UV–visible diffuse reflectance spectra of the sol–gel Ru catalyst with varying metal content treated at 70°C: (a) Ru-0.5, (b) Ru-1, and (c) Ru-2.

a sharp charge transfer band around 240 nm and a weak signal at approximately 325–350 nm. This charge transfer is undoubtedly due to the tendency of Ru to solvatize during its reaction with TEOS, forming $[RuCl_x(H_2O)_y]$ with $x + y = 6$.

In Fig. 7 these same catalysts are observed after calcination at 600°C. We now see a displacement of the charge transfer bands from 240 to 220 nm, the softening and displacement of the shoulders at 310 nm, and specially a sharp increase of the intensity of the 350 nm band. This increase is due to temperature and to metal content, indicating an interchange of the chlorine ligands of the precursor with the silanol groups during gelation. The hexacoordination of Ru is maintained even though it is distorted by the presence of $\equiv Si-O^-$ groups in its coordination sphere. In fresh gels, five bands are observed which may be assigned to electronic transitions from the σ and π orbitals from Cl to the T_{2g} orbital in Ru (see the corresponding discussion in (*1*)). They also point out to the formation of Ru –OH, $Ru-H_2O$, and $Ru-O-Si\equiv$ bonds, and they therefore imply a strong interaction between the Ru and the support through the silanol groups. They also may be related to the presence of OH and water groups on superficially located Ru sites.

The FTIR spectroscopic results are summarized in Fig. 8, showing the Ru-1 catalysts, treated at different temperatures. At 3484 cm^{-1} an asymmetric and rather intense band appears, to be assigned to an OH lengthening in the hydroxyl groups of the sample. This is supported by the fact that this band sharply diminishes in intensity. In fact the small band observed in the 600°C spectrum at 3600 cm^{-1} has no association with the OH lengthening at all. It is a typical signal for terminal silanol groups. They appear during calcination and may cause shifts in the microcrystallinity of the materials during calcination. They may also be related to the signals at 966 cm^{-1}, which in turn modifies its intensity during dehydroxilation. Furthermore a band is generated at 465 cm^{-1} due to the formation of oxygen bridges in the silica surface.

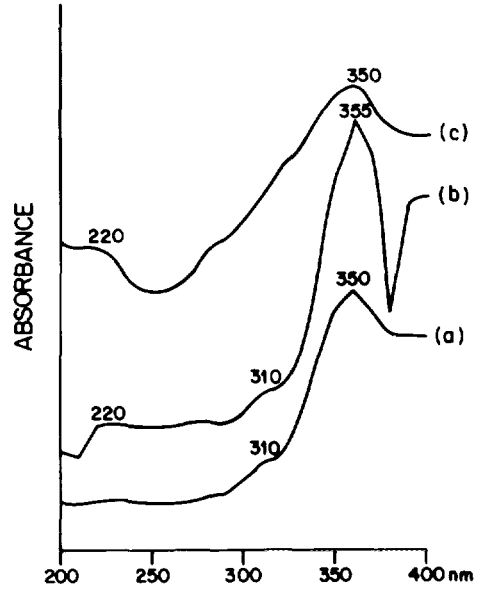

FIG. 7. UV–visible diffuse reflectance spectra of the sol–gel Ru catalyst with varying metal content treated at 600°C: (a) Ru-0.5, (b) Ru-1, and (c) Ru-2.

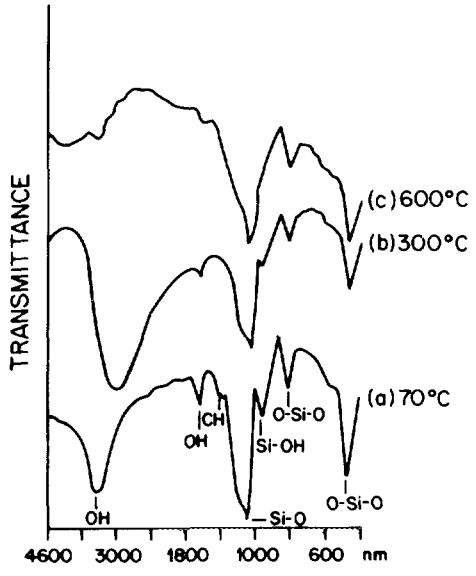

FIG. 8. Infrared spectra for the Ru-1 sol–gel catalyst at different temperatures.

In Fig. 9 we show the differential thermal (TGA) and thermogravimetric analyses (DTA) for the pure silica support. These curves reveal at 60°C a small endothermic peak as well as a 6% weight loss for the ruthenium-free silica. This is due to a water and EtOH desorption which were occluded in the gel after the gelation point. At this stage of postgelation, water and solvent are obtained as by-products of the reaction:

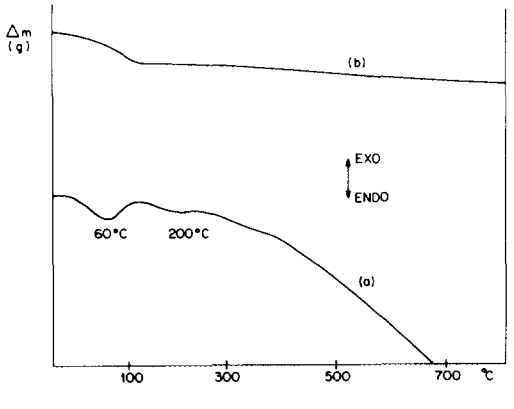

FIG. 9. DTA (a) and TGA (b) curves of the pure silica support.

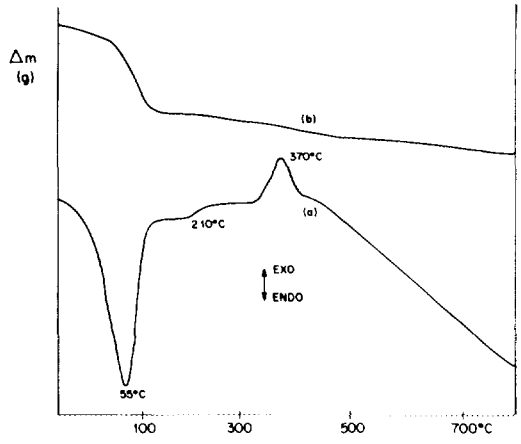

FIG. 10. DTA (a) and TGA (b) curves of the Ru-1 catalyst.

Hydrolysis

$$Si(EtO)_4 + H_2O \rightarrow (EtO)_3\text{—}Si\text{—}OH + EtOH.$$

Condensation

$$\equiv Si\text{—}OH + \equiv Si\text{—}OH \xrightarrow{RuCl_3 \cdot 3H_2O} [SiO_2]\text{—}Ru(OH)_xCl_y) + H_2O$$

$$\equiv Si\text{—}OEt + \equiv Si\text{—}OH \xrightarrow{RuCl_3 \cdot 3H_2O} [SiO_2]\text{—}[Ru(OH)_xCl_y] + EtOH,$$

where $x + y = 6$.

At 200°C another small endothermic peak is seen, which is due to the desorption of the residual alkoxide. At higher temperatures the silica structure remains stable. Here it is worth noting that this silica was prepared using the same conditions (pH = 9) as the corresponding ruthenium catalyst.

In Fig. 10 we report the DTA and TGA curves of the silica-supported Ru catalyst. Since these curves present large modifications from those in Fig. 9, it is clear that a rather strong effect is introduced by the metal in the support. At 55°C one can see a large endothermic peak as well as a 16% weight loss; these are due to water and solvent loss as well as a partial dehydroxylation on the catalyst. At 210°C another small endothermic peak is observed that should be

attributed to silicon-alkoxyde desorption which remained without reacting. One thing that should be pointed out is that, contrary to what we observed in pure silica (Fig. 9), in this case at 370°C an exothermic peak appears which is due to microcrystalline rearrangements in the ruthenium catalyst. The metal is incorporated to the silica network forming an octahedral structure (see Fig. 1), which is well in agreement with the theoretical results.

4. CATALYTIC ACTIVITY AND DEACTIVATION

The catalytic activity of Ru/SiO_2 has been thoroughly discussed before (*1*). We, however, present a brief summary here to be able to relate our new quantum mechanical and spectroscopic results to the peculiar characteristics of the sol–gel catalysts. In particular the Ru-0.5 sol–gel catalyst, is to be compared with traditionally impregnated catalysts with the same metal concentration (0.5% of Ru over SiO_2). The latter is impregnated over pure silica prepared with the same method and starting from TEOS at pH 9 and an area of 110 m^2/g. Firstly the areas are enormously different, being only 98 m^2/g for the impregnated Ru catalyst and 465 m^2/g for the sol–gel Ru-0.5. The increase of the exposed catalytic area does not diminish the activity by site, being 464 for the Ru-0.5 catalysts and 449 for Ru-impregnated gel. The main difference between the two catalysts lies in its resistance to deactivation.

The strong tendency of Ru to deactivate in hydrogenation reactions is probably due to the polymerization of partially hydrogenated species. The deactivation depends on the metallic particle size, this deactivation being faster for large particles (*26*). Ru-impregnated catalysts have particles with diameters of 66 Å; furthermore, the particle size is quite variable and difficult to control. On the contrary, in the sol–gel technique there is a much better control and particles under 30 Å are easy to obtain. In the case of Ru-0.5, for example, the deactivation constant during the hydrogenation of benzene is $K_{\text{sol-gel}}^{\text{Ru-0.5}} = 3.75$ showing clearly the advantage of the sol–gel preparation method. The Ru/SiO_2 (0.5%) catalysts prepared with traditional techniques in contrast has a benzene-hydrogenation deactivation constant of $K_{\text{impreg.}}^{0.5\%} = 153$, a factor almost 50 times higher. We now have elements to explain this remarkable resistance of sol–gel catalysts to deactivation.

Our new theoretical and spectroscopic results confirm the occlusion of most of the Ru in coordination complexes as that of Fig. 1. This is particularly true for the Ru-0.5 catalyst, although higher concentrations of metal (e.g., Ru-1 and Ru-2) can only have a certain amount of ruthenium in the silica network and the rest in the surface. The latter appear as $Ru–O_2$ groups but even these have a slower deactivation by coke formation than traditionally impregnated catalysts. This is due to the following reasons. Firstly the fact that Ru is at least partially occluded in the silica network for sol–gel catalysts while this is excluded for traditional impregnation. Furthermore we have seen from the spectroscopic evidence that Ru–OH and $Ru–H_2O$ groups are formed, meaning that the Ru is protected by these OH groups from the support. This is particularly true for superficial Ru which would then delay coke formation, being surrounded by these OH and H_2O groups. Finally the metal is incomparably more disperse in the sol–gel catalysts. Ru is so disperse in fact, to make coke formation very difficult even when it is in surface sites.

5. CONCLUSIONS

The above discussion about the remarkable resistance to catalytic deactivation presented by the sol–gel catalysts leads to several questions, each answered by a different aspect of our present theoretical and experimental results. The sol–gel Ru-0.5 catalyst was postulated (*1*) to have the Ru occluded in the silica network. What is its structure? This was answered by the *ab initio* SCF calculations which showed that the structure that surrounds the Ru with four SiO_4

tetrahedra, two coordinated by the vertex and two by the edges (Fig. 1), is more stable by 14 kcal/mol than the other most likely alternative (Fig. 2). Furthermore, the introduction of electronic correlation does not change the fact that the structure of Fig. 1 is the most stable (*21*). Another question raised in previous work (*2*) concerns the cause of the highly improved mechanical stability of the Ru/SiO_2 catalysts when they are prepared via the sol–gel technique. This is explained by the stability found for the structure of Fig. 1 both from the *ab initio* study and the EH calculations of the β-quartz structure containing Ru, which show a notable contraction of the silica structure produced by the occlusion of Ru in its midst. This confirms the image of the formation of a microporous solid with large BET surface areas and resistant to volatilization and sinterization already advanced in (*2*). The EH predictions on the contraction of the silica structure around Ru fit quite well with the X-ray results (*1*); the numbers in Table 2 give average Si–Si, O–Ru, and O–Si distances close to those observed.

Another question opened in (*1*) was on the sol–gel catalysts with higher Ru concentration, i.e., the Ru-1 and Ru-2, which have an important fraction of the Ru atoms on their surface, and are still quite resistant to deactivation. The UV–visible spectra reported here serve to explain this. Not only do the Ru-0.5, Ru-1, and Ru-2 diffuse reflectance spectra show similar bands, but also even after drying the Ru-1 catalyst has a strong signal related to $Ru–H_2O$ bonds. Even after calcination, the spectra show evidence of the existence of Ru–OH, $Ru–H_2O$, and Ru–O–Si$\equiv$ bonds. The strong interaction of Ru with the support via the silanol groups is then confirmed and furthermore the presence of OH and H_2O on the superficially located Ru is documented. This was assumed (*1*) to be the reason why the sol–gel prepared catalysts have a much slower deactivation rate than traditional catalysts. The presence of these OH and H_2O groups in Ru and the latter's strong binding to the silica surface clearly hinder the capacity of the polymerization of incompletely hydrogenated aromatic hydrocarbons, which is the number one cause of deactivation. This is reinforced by the fact that particle sizes are more controllable and substantially smaller when the sol–gel technique is used. Smaller particles are also less prone to deactivation.

All in all we see that the sol–gel catalysts have a series of fascinating properties both from a scientific and practical point of view and merit further research.

REFERENCES

1. López, T., Bosch, P., Asomoza, M., and Gómez, R., *J. Catal.* **133,** 247 (1992).
2. López, T., Herrera, L., Gómez, R., Zou, W., Robinson, K., and González, R. D., *J. Catal.* **136,** 621 (1992).
3. Poppe, E. J. A., and Mackenzie, J. D., *J. Non-Cryst. Solids* **106,** 236 (1988).
4. Teichner, S. J., Nicolaon, G. A. Vicarini, M. A., and Gardes, G. E. E. *Adv. Colloid Interface Sci.* **5,** 245 (1976).
5. López, T., López-Gaona, A., and Gómez, R., *J. Non-Cryst. Solids* **110,** 170 (1989).
6. López, T., López-Gaona, A., and Gómez, R., *Langmuir* **6,** 1443 (1990).
7. López, T., Villa, M., and Gómez, R., *J. Phys. Chem.* **95,** 1690 (1991).
8. Solymosi, F., *Catal. Rev.* **1,** 233 (1967).
9. Schwab, G. M., *Adv. Catal.* **27,** 1 (1978).
10. Bond, G. C., *in* "Metal Support and Metal Additive Effects in Catalysis" (B. Imelik *et al.*, Eds.) p. 1. Elsevier, Amsterdam, 1982.
11. King, D. L., *J. Catal.* **51,** 386 (1976).
12. Vannice, M. A., *J. Catal.* **37,** 449 (1975).
13. Cant, N. W., Hicks, P. C., and Lennon, B. S., *J. Catal.* **54,** 372 (1978).
14. Kubicka, H., *J. Catal.* **12,** 233 (1968).
15. Ekerdt, J. G., and Bell, A. T., *J. Catal.* **58,** 170 (1979).
16. Novaro, O., Chow, S., and Magnouat, Ph., *J. Catal.* **41,** 91 (1976).
17. Novaro, O., *Int. J. Quantum Chem.* **42,** 1047 (1992).
18. PSHF program written by J. P. Daudey, based on the original HONDO version. QCPE program No. 335 (1977). PSHF uses the relativistic pseudopotentials of Durand and Barthelat. Available on request from Laboratoire de Physique Quantique, Université Paul Sabatier, Toulouse, France.
19. Colmenares, F., Castillo, S., Martínez-Magadán,

J. M., Novaro, O., and Poulain, E., *Chem. Phys. Lett.* **189,** 378 (1992).
20. Hoffmann, R., *J. Chem. Phys.* **39,** 1397 (1963); Thorn, D. L., and Hoffmann, R., *J. Chem. Phys.* **39,** 1397 (1978).
21. Martínez-Magadán, J. M., work in progress.
22. López, T., Ramírez-Solís, A., and Novaro, O., *in* "Proceedings, XIII Ibero American Catalysis Congress, Segovia, Spain, July 1992," p. 695.
23. Novaro, O., *in* "Symmetry in Physics" (Frank and Wolf, Eds.), p. 61. (Springer-Verlag, Berlin/New York, 1992.
24. Dana, J. D., and Salisbury-Dana, E. S. "The System of Mineralogy," Vol. III, p. 251. Wiley, New York, 1962.
25. Wyckoff, "Crystal Structures," p. 312. Interscience, New York, 1960.
26. De Hartog, A. J., Deng, F., Jongerius, F., and Ponec, V., *J. Mol. Catal.* **60,** 99 (1990).